Impaired structural and functional regeneration of skeletal muscles from β2-adrenoceptor knockout mice

M. T. Silva,[1] L. A. Wensing,[2] P. C. Brum,[3] N. O. Câmara[2] and E. H. Miyabara[1]

1 Department of Anatomy, Institute of Biomedical Sciences, University of Sao Paulo, Sao Paulo, Brazil
2 Department of Immunology, Institute of Biomedical Sciences, University of Sao Paulo, Sao Paulo, Brazil
3 Department of Biodynamics, School of Physical Education and Sport, University of Sao Paulo, Sao Paulo, Brazil

The copyright line for this article was changed on 29th August, 2015 after original online publication.

Abstract

Aims: β2-adrenergic stimulation causes beneficial effects on structure and function of regenerating muscles; thus, the β2-adrenoceptor may play an important role in the muscle regenerative process. Here, we investigated the role of the β_2-adrenoceptor in skeletal muscle regeneration.

Methods: Tibialis anterior (TA) muscles from β2-adrenoceptor knockout (β_2KO) mice were cryolesioned and analysed after 1, 3, 10 and 21 days. The role of β2-adrenoceptor on regenerating muscles was assessed through the analysis of morphological and contractile aspects, M1 and M2 macrophage profile, cAMP content, and activation of TGF-β signalling elements.

Results: Regenerating muscles from β_2KO mice showed decreased calibre of regenerating myofibres and reduced muscle contractile function at 10 days when compared with those from wild type. The increase in cAMP content in muscles at 10 days post-cryolesion was attenuated in the absence of the β_2-adrenoceptor. Furthermore, there was an increase in inflammation and in the number of macrophages in regenerating muscles lacking the β2-adrenoceptor at 3 and 10 days, a predominance of M1 macrophage phenotype, a decrease in TβR-I/Smad2/3 activation, and in the Smad4 expression at 3 days, while akirin1 expression increased at 10 days in muscles from β_2KO mice when compared to those from wild type.

Conclusions: Our results suggest that the β2-adrenoceptor contributes to the regulation of the initial phases of muscle regeneration, especially in the control of macrophage recruitment in regenerating muscle through activation of TβR-I/Smad2/3 and reduction in akirin1 expression. These findings have implications for the future development of better therapeutic approaches to prevent or treat muscle injuries.

Keywords akirin1, contraction, macrophage, skeletal muscle regeneration, Smad, β2-adrenoceptor.

Mammalian skeletal muscles have an outstanding capacity to regenerate in response to damage. The muscle regeneration process includes coordinated steps of necrosis, inflammation and re-establishment of the structure and function of skeletal muscle tissue (Ciciliot & Schiaffino 2010, Ten Broek *et al.* 2010, Tsivitse 2010). After muscle damage, neutrophils are the inflammatory cells that initiate the invasion of the muscle tissue, followed by the classically activated or (M1) macrophages, which express CD86

and secrete pro-inflammatory cytokines, such as interleukin 1*β* (IL-1*β*), and inducible nitric oxide synthase (iNOS) (Locati *et al.* 2013, Mantovani *et al.* 2013). Subsequently, there is a shift in phenotype from M1 to alternatively activated M2 macrophages, which express the mannose receptor (CD206) and secrete anti-inflammatory cytokines, such as arginase-1 and found in inflammatory zone 1 (Fizz1) (Locati *et al.* 2013, Mantovani *et al.* 2013). Growth and repair of myofibres after injury are mediated by a resident population of mononuclear myogenic precursor cells, the satellite cells (SCs), which are small progenitor cells located between the basal lamina and the sarcolemma of individual muscle fibres (Ferrari *et al.* 1998). Following muscle injury, these cells divide and give rise to the SC progeny, the myoblasts, which fuse to each other to repair or replace damaged fibres (Blau *et al.* 1993, Boldrin *et al.* 2010).

Although the morphological aspects of skeletal muscle regeneration are well known, the molecular players involved in this process have not been fully elucidated. Accordingly, the signalling pathways that regulate protein turnover are strongly modulated over the course of this process (Drummond *et al.* 2009, Miyabara *et al.* 2010). The phosphoinositide 3-kinase (PI3K)/Akt/mechanistic target of rapamycin (mTOR) pathway and the ubiquitin proteasome system exert an essential role in skeletal muscle mass recovery after damage (Stipanuk 2007, Vary & Lynch 2007, Ge *et al.* 2009, Miyabara *et al.* 2010). Likewise, members of the transforming growth factor *β* (TGF-*β*) superfamily, such as myostatin, TGF-*β*1, TGF-*β*1 receptors (TGF-*β*-Rs), and their intracellular regulatory protein-receptor-regulated Smad2 and 3, and co-Smad, Smad4 are important to the success of muscle regenerative response (Droguett *et al.* 2010, Zhu *et al.* 2011). Furthermore, more recent studies have suggested the involvement of other factors, such as Mustn1 and akirin1, in the regulation of skeletal muscle regeneration, considering that Mustn1 is highly expressed during myoblast fusion (Krause *et al.* 2013), and akirin1 is strongly induced in activated satellite cells and macrophages (Salerno *et al.* 2009). The *β*2-adrenoceptor may play an important role in muscle regeneration, as several studies have shown that *β*2-adrenergic stimulation, through muscle treatment with *β*2-adrenergic agonists, increases the size and strength recovery of regenerating myofibres (Beitzel *et al.* 2004, 2007, Bricout *et al.* 2004, Ryall *et al.* 2008, Conte *et al.* 2012).

Skeletal muscle contains a significant proportion of *β*-adrenoceptors, of which the *β*2-subtype is the most prevalent (90%) (Kim *et al.* 1991). *β*-adrenoceptors belong to the guanine nucleotide-binding G protein-coupled receptor (GPCR) family. The classical *β*2-adrenoceptor signalling pathway through G*α*-AC-cAMP activation is, at least in part, responsible for the *β*2-adrenoceptor-mediated hypertrophy in the skeletal muscle (Navegantes *et al.* 2000, 2002, Hinkle *et al.* 2002). Once activated, cAMP can interact with the exchange protein directly activated by cAMP (EPAC) through the small GTPase Rap1, which may trigger the PI3K/AKT/mTOR signalling pathway, resulting in increased protein synthesis (Lynch & Ryall 2008). In addition, activated cAMP can bind to protein kinase A, which phosphorylates calpastatin, leading to the inhibition of the proteolytic activity of the calpain enzymes (Lynch & Ryall 2008). Furthermore, the G*βγ* dimer seems to activate the PI3K/AKT/mTOR signalling pathway, thereby contributing to muscle hypertrophy (Kline *et al.* 2007, Lynch & Ryall 2008).

Recently we have shown that *β*2-adrenergic stimulation, through formoterol treatment, is able to increase the size of regenerating myofibres in young and old rats through the activation of mTOR (Conte *et al.* 2012). In fact, previous studies have demonstrated that the *β*2-adrenergic agonists clenbuterol and fenoterol improved the recovery of myofibre size in regenerating skeletal muscles after transplantation (Roberts & McGeachie 1992) and muscle injury (Beitzel *et al.* 2004, Bricout *et al.* 2004). Additionally, other studies have indicated that *β*2-adrenoceptor stimulation contributes to the increase in satellite cell proliferation and differentiation (Roberts & McGeachie 1992, 1994, Spurlock *et al.* 2006), enrichment of vascular repair (Roberts & McGeachie 1994), decrease in inflammation and a more efficient restoration of the extracellular matrix (Pullar *et al.* 2008, Zhang *et al.* 2010). However, the role of the *β*2-adrenoceptor in skeletal muscle regenerative process and its importance to the muscle contractile recovery after injury is still unknown.

Considering that *β*2-adrenergic stimulation enhances the structural and functional repair of regenerating muscle, we hypothesized that the *β*2-adrenoceptor plays an important role in the skeletal muscle regenerative process. Therefore, this study aimed to investigate the role of the *β*2-adrenoceptor in histological, molecular and functional aspects of skeletal muscle regeneration of *β*2-adrenoceptor knockout (*β*₂KO) mice. To attain this goal, we evaluated morphological and muscle contractile aspects, M1 and M2 macrophage profile, cAMP content, activation of TGF-*β* signalling elements [TGF-*β* receptor I (T*β*R-I) and Smad2/3], and akirin1 and Smad4 expression in regenerating TA muscles from *β*₂KO mice.

Methods

All protocols used in this study were in accordance with Good Publishing Practice in Physiology (Persson 2013).

Animals

A cohort of male congenic Friend virus B-type (FVB) mouse strain lacking β2-adrenoceptor (β_2KO) (Chruscinski *et al.* 1999) and their age-matched FVB wild type (WT) controls at 2 months of age were used in this study. Mice were maintained in standard housing conditions (Conte *et al.* 2012).

Experimental design

In this study, one TA muscle (left hind limb) from each animal was subjected to cryolesion (Cryo group), and the contralateral TA muscle (right hind limb) was used as control (CL group). WT and β_2KO animals were randomized into four groups for the histological experiments ($n = 6$, each group). Both WT and β_2KO animals were subjected to cryolesion and were evaluated at 1, 3, 10 and 21 days post-cryolesion respectively. Contralateral muscles were designated as intact controls (CL group). In addition, distinct animals were used for the muscle contraction and cAMP quantification experiments and were evaluated at post-cryolesion day 10 (Conte *et al.* 2012).

Based on Pereira *et al.* (2014), animals were anesthetized and had the superior surface of the TA muscle entirely exposed. The cryolesion procedure was performed according to Conte *et al.* (2012), using the iron rod (flat end) dimensions of 2×9 mm and bringing it into contact with the muscle twice (i.e., in the two longitudinal halves of the muscle).

Histology

Animals were killed by decapitation, after which their left and right TA muscles were removed, weighed and stored according to Pereira *et al.* (2014). Muscle cross sections (10-μm-thick) obtained from the TA middle-bellies were stained with an aqueous solution of toluidine blue and borax (Miyabara *et al.* 2004). Necrotic myofibres were localized by histochemical detection of lysosomal acid phosphatase activity (Gomori lead method) (Bancroft 1996, Miyabara *et al.* 2010).

The stained sections were analysed in a Nikon Eclipse light microscope (PCM2000; Nikon, New York, NY, USA), and figures were prepared using ADOBE PHOTOSHOP 7.0 (Adobe Systems, San Jose, CA, USA).

Cyclic AMP (cAMP) quantification

cAMP quantification was performed according to Conte *et al.* (2012).

Antibodies for immunostaining

The primary antibodies used for immunostaining were (1) mouse monoclonal anti-MAC387 (macrophage) (1 : 200; cat# ab22506; Abcam, Cambridge, MA, USA), (2) rabbit polyclonal anti-TGF-β receptor I phospho S165 (cat# ab112095, 1 : 250; Abcam) and (3) rabbit monoclonal anti-Smad2/3 (cat# 8685; 1 : 200; Cell Signaling Technology, Danvers, MA, USA). The corresponding secondary antibodies used were (1) goat anti-mouse IgG-fluorescein isothiocyanate (FITC) (1 : 200; cat# 115-095-166; Jackson ImmunoResearch Laboratories, Baltimore, PA, USA); and (2) goat anti-rabbit IgG-rhodamine (1 : 200; cat# ab6718; Abcam).

Immunostaining

Muscle cross sections were immunostained according to Pereira *et al.* (2014).

Photomicrographs of the stained sections were obtained using a fluorescence microscope equipped with a 20× magnification objective lens (Nikon, Eclipse E1000, ACT-1 version 2.2 or Observer D1; Zeiss; Jena, Germany), and with FITC, Rhoda mine and fura filters.

Antibodies for Western blotting

The primary antibodies used for Western blotting were (1) rabbit polyclonal anti-Smad4 (1 : 1000; cat# 9515; Cell Signaling Technology), (2) rabbit polyclonal anti-akirin1 (1 : 1000; cat# ab77075; Abcam) and (3) rabbit polyclonal anti-glyceraldehyde-3-phosphate dehydrogenase (GAPDH) (1 : 2000; cat# ABS16; Millipore, Temecula, CA, USA). The corresponding secondary antibody used for all Western blots was peroxidase-conjugated AffiniPure goat anti-rabbit IgG (1 : 10 000; cat# 111-035-003; Jackson Immuno Research Laboratories).

Western blot analysis

Western blot analysis was executed according to Conte *et al.* (2012). Densitometry analysis was performed based on Pereira *et al.* (2014).

Gene expression analysis

Reverse transcription. Total RNA was isolated from muscle samples using Trizol reagent (Invitrogen,

Carlsbad, CA, USA). Reverse transcription was performed according to Silva *et al.* (2012).

Primer design. The following primer sequences were used: Fizz-1: 5′-GAGACCATAGAGATTATCGTGG A-3′ forward, 5′-CACACCCAGTAGCAGTCATC-3′ reverse; Arginase-1: 5′-CAATGAAGAGCTGGCTGGT GT-3′ forward, 5′- GTGTGAGCATCCACCCAAATG-3′ reverse; iNOS: 5′-CTGCAGCACTTGGATCAG-3′ forward, 5′-CGTACCAGGCCCAATGAG-3′ reverse; IL-1β: 5′-CCAAAAGATGAAGGGCTGCTTCC-3′ forward, 5′-GGATGGGCTCTTCTTCAAAGATG-3′ reverse and TFIID: 5′-TTAGGCCTGGAAAGGTGTTA CG-3′ forward, 5′-CCTCCAAACAGATGGAACAT TCT-3′ reverse.

Primer sequences for Fizz-1, Arginase-1, iNOS were obtained from Villalta *et al.* (2011) and primer sequences for IL-1β and the transcription factor IID (TFIID) were obtained from Acharyya *et al.* (2007) and Silva *et al.* (2012) respectively. The primers were synthesized from Exxtend Biotecnologia, Brazil.

Real-time PCR. Real-time PCR was carried out on an ABI Prism 7300 Sequence detection system (QuantStu- dio™ 12K Flex Real-Time PCR System; Applied Bio- systems, Foster City, CA, USA) according to Aoki *et al.* (2009). The transcription factor TFIID was used as the housekeeping gene. Expression values are reported as fold difference relative to the expression of the control (calculated as $2^{-\Delta\Delta C_t}$). The WT Cryo 1d group was used as control when no amplification was detected in WT CL group.

In addition to 3 and 10 days post-injury, the time point of day 1 was included in the gene expression analysis of the M1 and M2 macrophage markers, con- sidering that M1 macrophages invade the wound site at 1 day post-damage (Turner & Badylak 2012).

Flow cytometry

Muscle samples underwent two enzymatic dissociations and, subsequently, the cells were filtered with a 40-μm cell strainer (BD Biosciences, San Jose, CA, USA) (Che- ung *et al.* 2012). Based on Larocca *et al.* (2013), the fil- trate was centrifuged at 600 *g* for 15 min and cells were resuspended in lyses buffer for erythrocytes removal. Cell pellets were resuspended in PBS supple- mented with 2% foetal bovine serum and stained with the following antibodies at 1 : 100 dilution for 30 min at 4 °C in the dark: APC-Cy7-conjugated anti-CD11b, PE-conjugated anti-CD86 (for validation of M1 polari- zation) and APC-conjugated anti-CD206 (for validation of M2 polarization). At least 50 000 cells were acquired with BD FACSCanto II using the FACSDiva software (BD Biosciences). The data analysis was performed with

FlowJo software (Tree Star, Ashland, OR, USA). A gate for macrophages was set based on forward scatter (FSC) and CD11b positive. From this population, gates for CD86 and CD206 positive cells were created. Results were present as the percentage of positively stained cells within the cell population (macrophages gate) or macrophage population (CD86 and CD206 gates). The results are representative of 3 distinct experiments.

Mechanical measurements

Mechanical measurements in TA muscles were obtain- ed according to Pereira *et al.* (2014). Frequencies of isolated twitches, maximum tetanic contraction and tet- anus during fatigue protocol were 0.2, 200 and 100 Hz respectively.

Quantitative and morphometric analyses

ImagePro Plus software (Media Cybernetics, Silver Spring, MD, USA) was used for the quantitative and morphometric analyses.

Myofibre CSA was manually measured, and it was obtained from all regenerating myofibres with central- ized nuclei in muscles analysed on post-cryolesion day 10 and 21 (Pereira *et al.* 2014).

Necrotic myofibres in three whole cross sections for each muscle (*n* = 3) stained with acid phosphatase and analysed on post-cryolesion day 1 were counted and expressed as the percentage of total myofibres.

Regenerating myofibres were counted and expressed as the percentage of total myofibres according to Conte *et al.* (2012).

The areas of inflammation in the muscle cross sec- tions stained with toluidine blue and analysed on post-cryolesion days 3 and 10 were measured and expressed as the percentage of the whole muscle cross section (*n* = 4 per group).

Macrophages were quantified based on Pereira *et al.* (2014).

The TβR-I positive area and the number of nuclei positive for Smad2/3 were obtained from the injured muscle area of the whole muscle cross sections analy- sed at 3 days post-cryolesion (*n* = 3, each group). Subsequently, the injured area and the whole muscle cross-section area were measured. The TβR-I positive area was expressed as the percentage of the entire muscle cross section, and the incidence of Smad2/3 positive nuclei was expressed as the number of Smad2/3 positive nuclei per square millimetre.

Statistical analysis

Multiple comparisons of mean values were performed according to Conte *et al.* (2012). The unpaired *t*-test

was used for comparisons between two groups (Miyabara *et al.* 2010). For all comparisons, $P \leq 0.05$ was considered significant.

Results

Body and muscle weights

The body weight of WT mice was not altered over the course of 21 days (Table 1), whereas the body weight of β_2KO mice increased 8% at 10 days and 12% at 21 days ($P \leq 0.05$; Table 1).

At 1 day post-cryolesion, muscle weight of both WT and β_2KO mice increased, when compared with the respective contralateral group (47 and 37% respectively; $P \leq 0.05$; Table 1), but muscle weight of β_2KO mice increased 13% less than that of WT mice, in the same period ($P \leq 0.05$; Table 1). On post-cryolesion day 3, muscle weight of both WT and β_2KO mice decreased, when compared with muscles on post-cryolesion day 1 (28 and 27%, respectively, $P \leq 0.05$; Table 1). However, muscle weight was unchanged when compared to the respective contralateral groups (Table 1).

When analysed at 10 days, muscle weight of WT mice decreased by 24%, when compared to its respective contralateral group ($P \leq 0.05$; Table 1), whereas it was unaltered in β_2KO mice. On post-cryolesion day 21, muscle weight of WT mice increased by 35%, when compared with that on post-cryolesion day 10 ($P \leq 0.05$; Table 1), until it reached a value similar to the respective contralateral group (Table 1). By contrast, muscle weight of β_2KO mice remained unchanged at 10 and 21 days post-cryolesion (Table 1).

Histology

Histological cross sections of TA muscle samples collected on post-cryolesion days 1, 3, 10 and 21 were stained with toluidine blue and analysed by light microscopy. Intact contralateral muscles from both WT and β_2KO mice exhibited polygonal fibres with peripheral nuclei, which is typical of normal tissue structure (Fig. 1).

Contralateral muscles from β_2KO mice had slightly smaller myofibre CSAs when compared to muscles from WT mice, that is, 59% of myofibres were smaller than 2000 μm^2 in the contralateral β_2KO group, whereas 54% of myofibres were smaller than 2000 μm^2 in the contralateral WT group ($P \leq 0.05$; Fig. 1).

On post-cryolesion day 1, tissue damage in both WT and β_2KO mice was evident in freeze-injured TA muscles, as confirmed by the presence of hypercontracted fibres, inflammatory cell infiltration and clear spaces between the cells, indicating myonecrosis, tissue disruption and oedema (Fig. 1). In addition, the percentage of necrotic myofibres in muscles analysed on post-cryolesion day 1 from both WT and β_2KO mice was similar (43 ± 9 and 44 ± 11%, respectively, Fig. 1).

At 3 days post-cryolesion, a small inflammatory area was evident in muscles from both WT and β_2KO mice (18 ± 3 and 25 ± 4% of the entire muscle cross section, respectively, Fig. 1), with a tendency of increase in muscles from β_2KO mice compared to those from WT mice (Fig. 1). Hypercontractured myofibres were also observed in β_2KO mice (Fig. 1), suggesting the persistence of acute signs of injury.

At 10 days post-cryolesion, 69.5% of myofibres containing central nuclei from WT mice were smaller than 1200 μm^2, against only 15% in the contralateral group ($P \leq 0.05$; Fig. 1). Additionally, the regenerating muscles from WT group showed split fibres. At the same time point, regenerating myofibres with central nuclei from β_2KO mice were smaller than those from the contralateral group (74%

Table 1 Comparison of body (BW, g) and muscle weight (MW, mg) from cryolesioned groups from wild-type (WT) and β_2-adrenoceptor knockout (β_2KO) mice

	Groups	C		Cryo 1d		Cryo 3d		Cryo 10d		Cryo 21d
BW (g)	WT	27.4 (1.3)		27.5 (1.3)		28.1 (0.8)		28.3 (1.4)		29.1 (1.4)
	β_2KO	26.6 (1.2)		26.7 (1.2)		27.4 (1.2)		28.7 (1.8)*		29.8 (2.0)*

	Groups	CL 1d	Cryo 1d	CL 3d	Cryo 3d	CL 10d	Cryo 10d	CL 21d	Cryo 21d
MW (mg)	WT	36.6 (0.7)	53.8 (1.1)*	36.6 (1.9)	38.6 (3.2)[a]	35.8 (0.8)	27.2 (2.0)*[ab]	38.9 (1.8)	36.6 (1.3)[ac]
	β_2KO	34.3 (1.0)	46.9 (2.5)*[#]	39.1 (1.0)	34.4 (3.9)[a]	39.0 (4.1)	34.0 (4.2)[#a]	39.1 (1.1)	38.2 (2.3)[a]

Values are expressed as means and SD; $n = 6$. ANOVA followed by the Bonferroni's test for multiple comparisons was applied to test differences among the various groups. BW, body weight; MW, muscle weight; C, intact control, Cryo 1d, Cryo 3d, Cryo 10d, and Cryo 21d, cryolesioned and analysed after 1, 3, 10 and 21 days; CL, intact muscle from the contralateral leg, respectively.
*$P \leq 0.05$ vs. matched control or matched CL.
[#]$P \leq 0.05$ vs. the matched group from WT; [a]$P \leq 0.05$ vs. Cryo 1d; [b]$P \leq 0.05$ vs. Cryo 3d; [c]$P \leq 0.05$ vs. Cryo 10d.
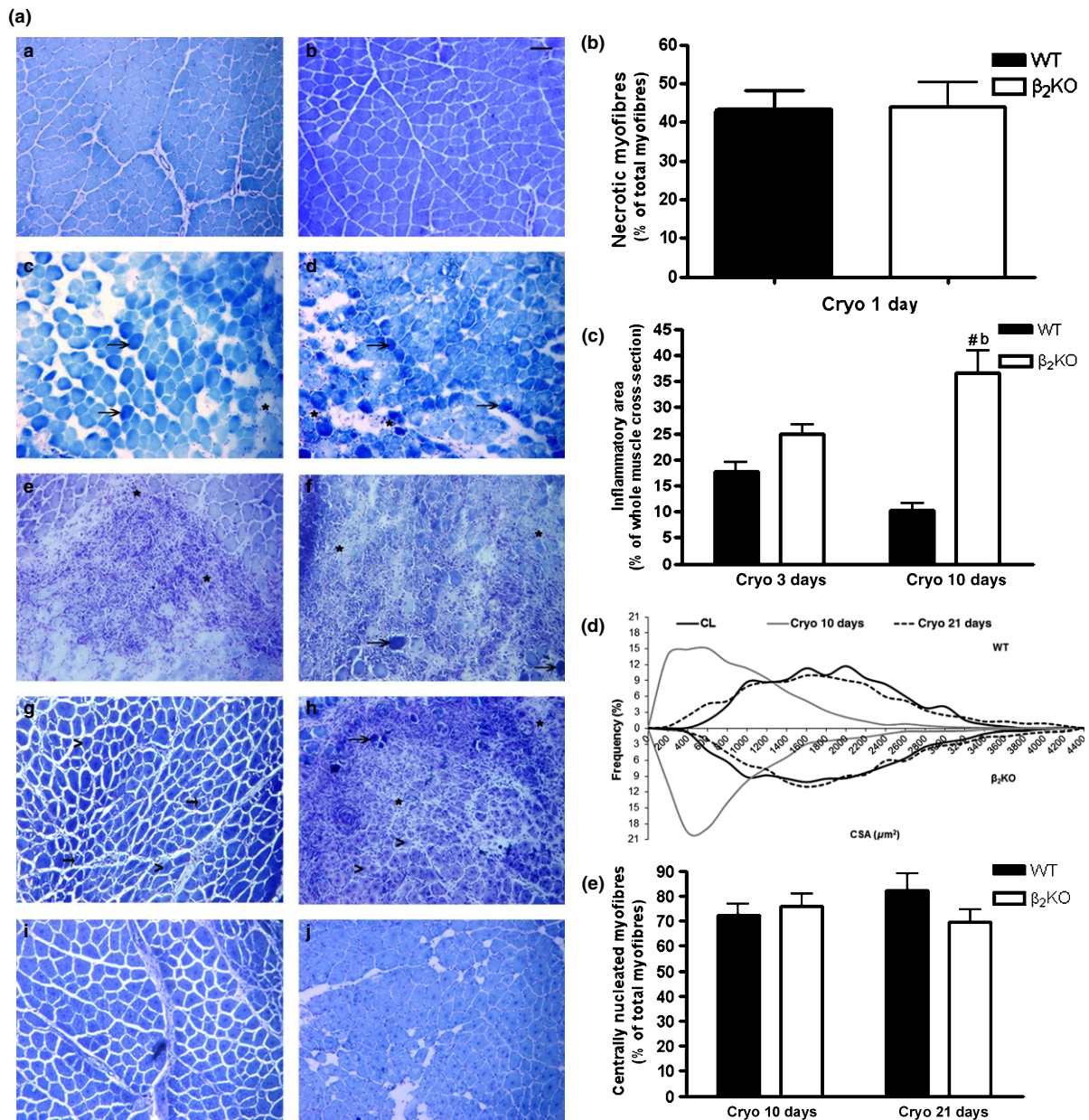
Figure 1 (a) Representative toluidine blue stained tibialis anterior (TA) muscle cross sections of WT and $β_2$KO mice. (a) WT contralateral group; (b) KO contralateral group; (c) WT, 1 day post-cryolesion; (d) $β_2$KO, 1 day post-cryolesion; (e) WT, 3 days post-cryolesion; (f) $β_2$KO, 3 days post-cryolesion; (g) WT, 10 days post-cryolesion; (h) $β_2$KO, 10 days post-cryolesion; (i) WT, 21 days post-cryolesion; (j) $β_2$KO, 21 days post-cryolesion. Arrows, hypercontracted fibres; asterisks, inflammatory cell infiltration; arrow head, cells with centralized nuclei; small arrows, split fibres. Bar: 50 μm. (b) Comparison of percentage of necrotic myofibres in muscles from WT and $β_2$KO mice at 1 day post-cryolesion (% of total myofibres from whole muscle CSA). Data are expressed as mean and SD; n = 3. (unpaired *t*-test). (c) Comparison of percentage of inflammatory area in muscles from WT and $β_2$KO mice at 3 and 10 days post-cryolesion (% of whole muscle CSA). Data are expressed as mean and SD; n = 4. (analysis of variance followed by Bonferroni's test for multiple comparisons) [#]$P ≤ 0.05$ vs. WT mice; [b]$p ≤ 0.05$ vs. Cryo 3d. (d) Frequency distribution of myofibre cross-sectional area (CSA) in contralateral and cryolesioned muscles from WT and $β_2$KO mice analysed at 10 and 21 days post-cryolesion; n = 5. Kolmogorov–Smirnov test was applied in order to test differences between groups. (e) Comparison of percentage of centrally nucleated myofibres in muscles from WT and $β_2$KO mice at 10 and 21 days post-cryolesion (% of total myofibres from whole muscle CSA). Data are expressed as mean and SD; n = 3. (analysis of variance followed by Bonferroni's test for multiple comparisons).

were smaller than 1200 μm^2 in the β_2KO group, against 21% in the contralateral group, $P \leq 0.05$; Fig. 1) and from WT mice (54% in β_2KO vs. 62% in WT, with CSA values between 400 and 1200 μm^2 respectively; $P \leq 0.05$; Fig. 1). Also, muscles from the β_2KO group exhibited typical signs of acute lesion, such as hypercontracted fibres and inflammatory infiltration, which was larger compared to that from the WT group (254%, $P \leq 0.05$; Fig. 1). In addition, the area of inflammation increased in muscles from the β_2KO group analysed on post-cryolesion day 10, when compared to those analysed on post-cryolesion day 3 (47%, $P \leq 0.05$; Fig. 1). However, the area of inflammation was unchanged in the WT group (Fig. 1).

On post-cryolesion day 21, TA muscles from freeze-injured WT mice were completely regenerated, as evidenced by the classical signs of regeneration (Karpati *et al.* 1988), that is, restored myofibres with centralized nuclei, CSA values similar to contralateral muscles, as well as split fibres (Fig. 1). At this same time point, regenerating myofibres from β_2KO mice were larger than those from the Cryo 10d group (74% were larger than 1200 μm^2 in the β_2KO group, $P \leq 0.05$; Fig. 1) and from WT mice (74% were larger than 1200 μm^2 in the β_2KO group, $P \leq 0.05$; Fig. 1). In addition, cryolesioned muscles analysed at 21 days post-injury from β_2KO mice had regenerating myofibres with centralized nuclei with similar calibre size, when compared to those from WT mice (Fig. 1).

The percentage of regenerating myofibres with centralized nuclei was unaltered in the groups analysed on post-cryolesion days 10 and 21 (Fig. 1).

Total number of macrophages and muscle macrophage phenotype

Incidence of Mac387 positive macrophages. At 3 and 10 days post-cryolesion, the number of macrophages in muscles from WT and β_2KO mice increased when compared to the respective controls (WT: 4978 and 3988% respectively; β_2KO: 10 038 and 8572% respectively; $P \leq 0.05$; Fig. 2). In addition, at 3 and 10 days post-cryolesion, the number of macrophages in muscles from β_2KO mice was 157 and 173% higher than that observed in muscles from WT mice respectively ($P \leq 0.05$; Fig. 2).

M1 and M2 associated genes. Gene expression of IL-1β and arginase-1 did not change in all groups evaluated (Fig 3).

iNOS mRNA expression did not change in muscles from WT group evaluated at 1, 3 and 10 days post-cryolesion, when compared to the respective
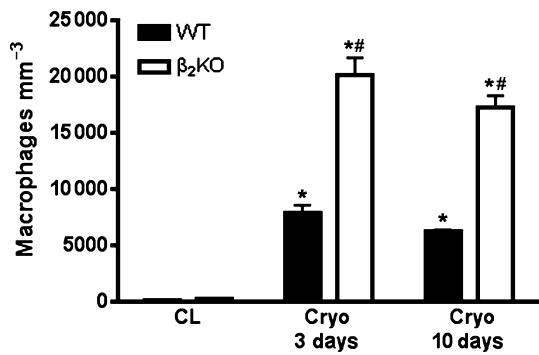

Figure 2 Incidence of macrophages per cubic millimetre (mm^3) of contralateral (CL) muscles and injured muscles analysed on post-cryolesion days 3 and 10 (Cryo 3d; Cryo 10d) from WT and β_2KO mice. Data are expressed as mean and SD; $n = 3$. (analysis of variance followed by Bonferroni's test for multiple comparisons) *$P \leq 0.05$ vs. CL; #$P \leq 0.05$ vs. WT mice.

contralateral muscles (Fig 3). On day 1 post-cryolesion, iNOS mRNA expression in muscles from β_2KO group increased 705% when compared to that of the contralateral muscles, and 1116% when compared to that from WT group, evaluated in the same time point post-injury ($P \leq 0.05$; Fig. 3). By contrast, iNOS mRNA expression in muscles from β_2KO group decreased at 3 and 10 days post-cryolesion when compared to that obtained on day 1 post-cryolesion (89 and 82% respectively; $P \leq 0.05$; Fig. 3).

Fizz-1 mRNA expression was unaltered in muscles from WT group in all time points analysed (Fig. 3). Fizz-1 mRNA expression increased in the contralateral muscles from β_2KO group, when compared to that from the contralateral muscles from WT group (1238%, $P \leq 0.05$; Fig. 3). By contrast, Fizz-1 mRNA expression decreased in the injured muscles at 1, 3 and 10 days post-injury when compared to that obtained in the contralateral muscles from β_2KO group (96, 99 and 92%, respectively, $P \leq 0.05$, Fig. 3).

CD11b^{+ve}, CD86^{+ve} and CD206^{+ve} cell population. The CD11b^{+ve} population increased in regenerating muscles from both WT and β_2KO mice analysed at 3 and 10 days when compared to the respective controls (WT: 557 and 286% respectively; $P \leq 0.05$; β_2KO: 459 and 419%, respectively, $P \leq 0.05$; Fig. 4), and this increase was more pronounced in muscles from β_2KO mice when analysed at 3 days (46%, $P \leq 0.05$; Fig. 4), but not at 10 days.

The percentage of CD86^{+ve} cells in the CD11b^{+ve} population in muscles from WT and β_2KO mice analysed at 3 and 10 days did not change in any of the groups evaluated. However, the percentage of
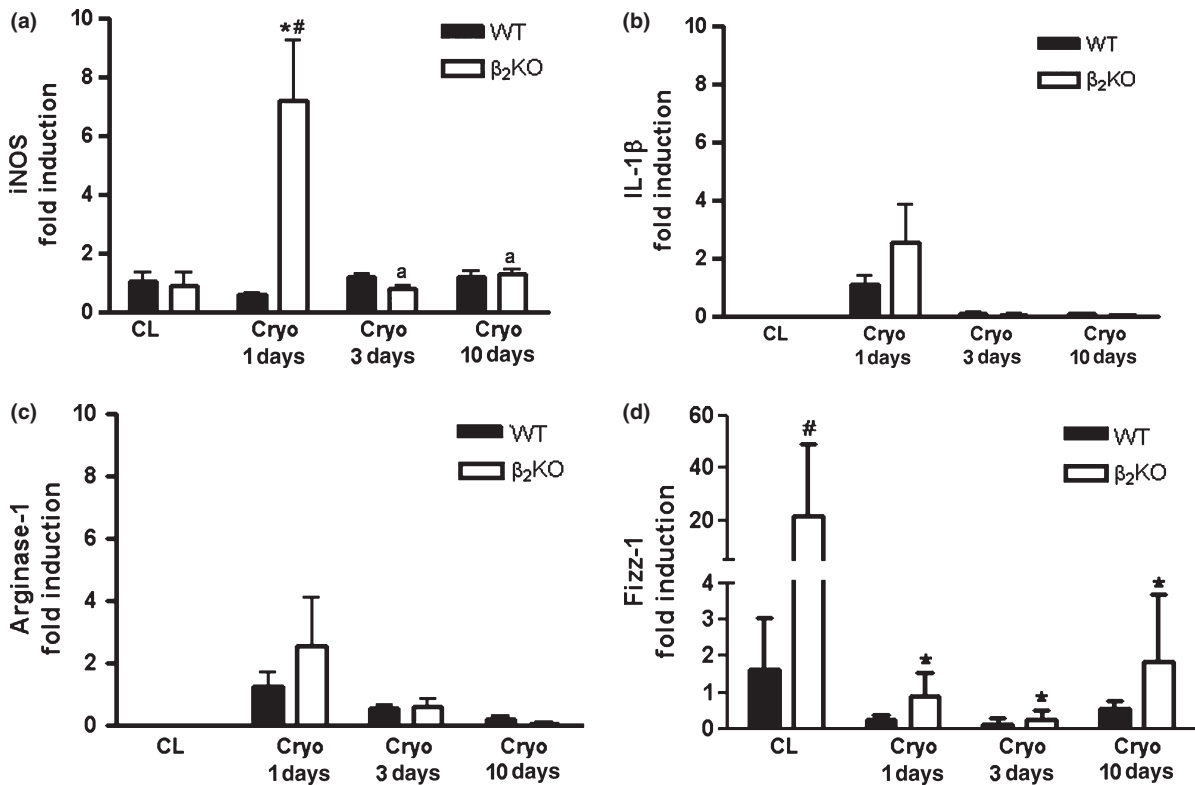
Figure 3 iNOS (a) IL-1*β*, (b) arginase-1, (c) fizz-1 and (d) gene expression analysed 1, 3 and 10 days after cryolesion in WT and *β*2KO mice. Values are expressed as mean and SD; n = 4–5 (analysis of variance followed by Bonferroni's test for multiple comparisons) *$P \leq 0.05$ vs. matched CL; #$P \leq 0.05$ vs. matched WT group; [a]$p \leq 0.05$ vs. Cryo 1d.

CD86[+ve] cells tended to increase in the CD11b[+ve] population in regenerating muscles from *β*2KO mice, when compared to those from WT mice at the same time point evaluated (Fig. 4).

The percentage of CD206[+ve] cells in the CD11b[+ve] population in regenerating muscles from WT and *β*2KO mice analysed at 3 and 10 days decreased when compared to the respective contralateral muscles (WT: 96 and 50% respectively; $P \leq 0.05$; *β*2KO: 94 and 47%, respectively, $P \leq 0.05$; Fig. 4).

Activation of T*β*R-I/Smad2/3

With regard to the immunostaining against T*β*R-I, contralateral muscles from both WT and *β*2KO mice did not present immunopositivity for T*β*R-I (data not shown). The area positive for T*β*R-I in injured muscles from *β*2KO mice was 64% smaller than that from WT mice at the same time point evaluated ($P \leq 0.05$; Fig. 5). Similarly, nuclei positive for Smad2/3 were not observed in contralateral muscles from either WT or *β*2KO mice (data not shown). Also, at 3 days post-cryolesion, 28% fewer nuclei were positive for Smad2/3 in muscles from *β*2KO mice, compared to muscles from WT mice at the same time point evaluated ($P \leq 0.05$; Fig. 6).

Smad4 and akirin1 expression in regenerating muscles

At 3 days post-cryolesion, Smad4 expression decreased in injured muscles from WT and *β*2KO mice when compared to their controls (25 and 41% respectively; $P \leq 0.05$; Fig. 7) and this decrease was more pronounced in muscles from *β*2KO mice when compared to those from WT group (32%; $P \leq 0.05$; Fig. 7). At 10 days post-cryolesion, Smad4 expression decreased at the same rate in injured muscles from both WT and *β*2KO mice, when compared to their controls (29 and 25% respectively; $P \leq 0.05$; Fig. 7). Moreover, the Smad4 expression in contralateral muscle from *β*2KO mice decreased when compared to contralateral muscle from WT group (24%; $P \leq 0.05$; Fig. 7).

Akirin1 expression was not detected in contralateral muscles from either WT or *β*2KO groups (Fig. 7), but it was highly expressed at 10 days post-cryolesion in muscles from WT and *β*2KO mice when compared to their respective controls (1931 and 2387% respectively; $P \leq 0.05$; Fig. 7). In addition, the akirin1 expression in injured muscle from *β*2KO mice analysed on post-cryolesion day 10 was more robust when compared with that in injured muscles from WT mice (95%; $P \leq 0.05$; Fig. 7).
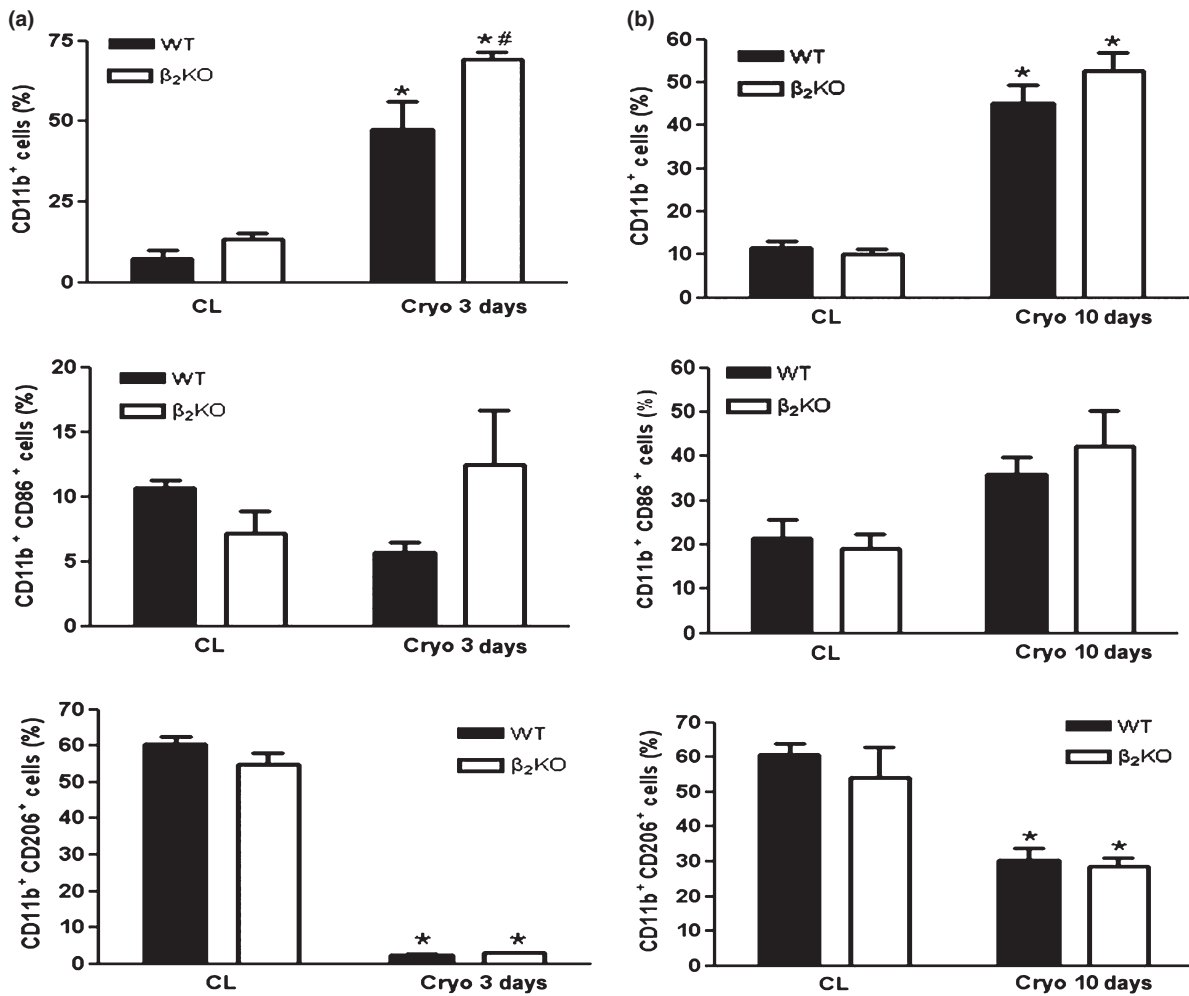
Figure 4 CD11b^{+ve}, CD86^{+ve} and CD206^{+ve} cell population. (a) Percentage of CD11b^{+ve} population, CD86^{+ve} and CD206^{+ve} cells in the CD11b^{+ve} population in contralateral and injured muscles analysed at 3 days from both WT and $β_2$KO mice. (b) Percentage of CD11b^{+ve} population, CD86^{+ve} and CD206^{+ve} cells in the CD11b^{+ve} population in contralateral and injured muscles analysed at 10 days from both WT and $β_2$KO mice. Values are expressed as mean and SD; n = 3–5 (analysis of variance followed by Bonferroni's test for multiple comparisons) *$P ≤ 0.05$ vs. CL; #$P ≤ 0.05$ vs. WT mice.

cAMP levels in regenerating muscles

We investigated whether disruption of the $β2$-adrenoceptor gene target would decrease cAMP levels in contralateral and injured muscles and whether cryolesion by itself would change such levels in muscles from both WT and $β_2$KO mice. No changes were observed in cAMP levels in contralateral muscles from WT and $β_2$KO mice (Fig. 8). As expected, cryolesion alone induced a 228% increase in cAMP levels in muscles from WT mice after 10 days, when compared to their controls ($P ≤ 0.05$; Fig. 8). In addition, the increase in cAMP levels was attenuated in TA muscles from $β_2$KO mice at the same time point, when compared to their controls (125%, $P ≤ 0.05$; Fig. 8).

Maximum tetanic and specific forces, and resistance to fatigue

The influence of the $β2$-adrenoceptor on the functional recovery of freeze-injured muscles was evaluated through the analysis of *in vivo* muscle contraction measurements on post-cryolesion day 10.

At the pre-fatigue tetanic contraction measurement, the absolute and specific force decreased by 34 and 43%, respectively, in the cryolesioned muscles from WT mice, when compared to the contralateral muscles from WT mice ($P ≤ 0.05$, Fig. 9). Likewise, the tetanic force and specific force decreased by 43 and 27%, respectively, in the injured muscles from $β_2$KO mice, when compared to the contralateral muscles from $β_2$KO mice ($P ≤ 0.05$, Fig. 9). Contralateral muscles
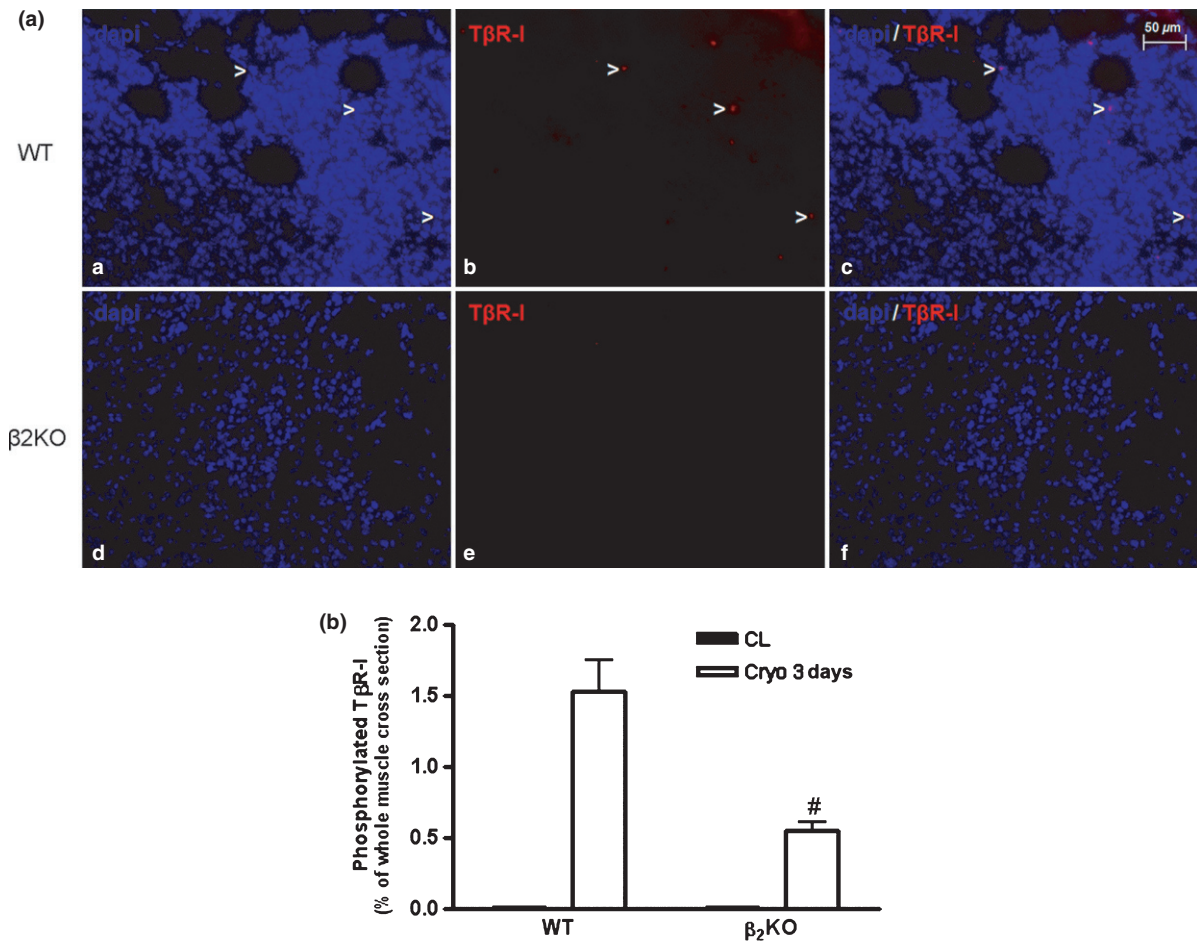
(a)

(b)

Figure 5 Active/phosphorylated TβR-I positive areas in muscle cross sections. (a) Immunostaining for active/phosphorylated TβR-I in tibialis anterior (TA) muscle cross sections. TA muscles from WT and β_2KO mice at 3 days post-cryolesion. (a and d) DAPI (blue; stained nuclei) in muscles from WT and β_2KO mice respectively; (b and e) muscles immunostained for phosphorylated TβR-I (red; TGF-β RI) from WT and β_2KO mice respectively; (c and f) co-staining for TGF-β RI and DAPI in muscles from WT and β_2KO mice respectively. Arrow heads indicate muscle areas immunopositive for phosphorylated TβR-I. (b) Comparison of percentage of activated/phosphorylated TβR-I positive muscle cross-sectional areas (% of whole muscle CSA) in contralateral muscles (CL) and regenerating muscles at 3 days post-cryolesion (Cryo 3d) in WT and β_2KO mice. Data are expressed as mean and SD; $n = 3$ (analysis of variance followed by Bonferroni's test for multiple comparisons) $^{\#}P \leq 0.05$ vs. WT mice.

from β_2KO mice showed a 17% decrease in absolute force and a 29% decrease in specific force, when compared to those from WT mice ($P \leq 0.05$, Fig. 9). Similarly, injured muscles from β_2KO mice showed 18% lower tetanic force and 17% lower specific force, compared to those from WT mice ($P \leq 0.05$, Fig. 9).

Regarding the post-fatigue tetanic and specific forces, we observed a reduction in tetanic and specific forces in injured TA muscles from WT and β_2KO mice when compared to their controls (WT mice: 42 and 40% respectively; β_2KO mice: 43 and 24% respectively; $P \leq 0.05$, Fig. 9). Similarly to the pre-fatigue tetanic contraction measurement, contralateral and injured muscles from β_2KO mice showed lower tetanic and specific force, when compared to those from WT mice (contralateral muscles: 24 and 34%

decrease respectively; cryolesioned muscles: 26 and 16% decrease respectively; $P \leq 0.05$, Fig. 9).

The post-fatigue tetanic and post-fatigue specific forces decreased, when compared to the pre-fatigue tetanic and pre-fatigue specific forces, in both WT and β_2KO mice (contralateral muscles from WT mice: 11 and 9% decrease respectively; cryolesioned muscles from WT mice: 10 and 13% decrease respectively; contralateral muscles from β_2KO mice: 20 and 16% decrease respectively; cryolesioned muscles from β_2KO mice: 19 and 13% decrease respectively; $P \leq 0.05$, Fig. 9).

Tibialis anterior muscle strength was measured at four time points during the fatigue protocol (1st, 4th, 7th and 10th contractions). In contralateral muscles from both WT and β_2KO mice, there was a significant
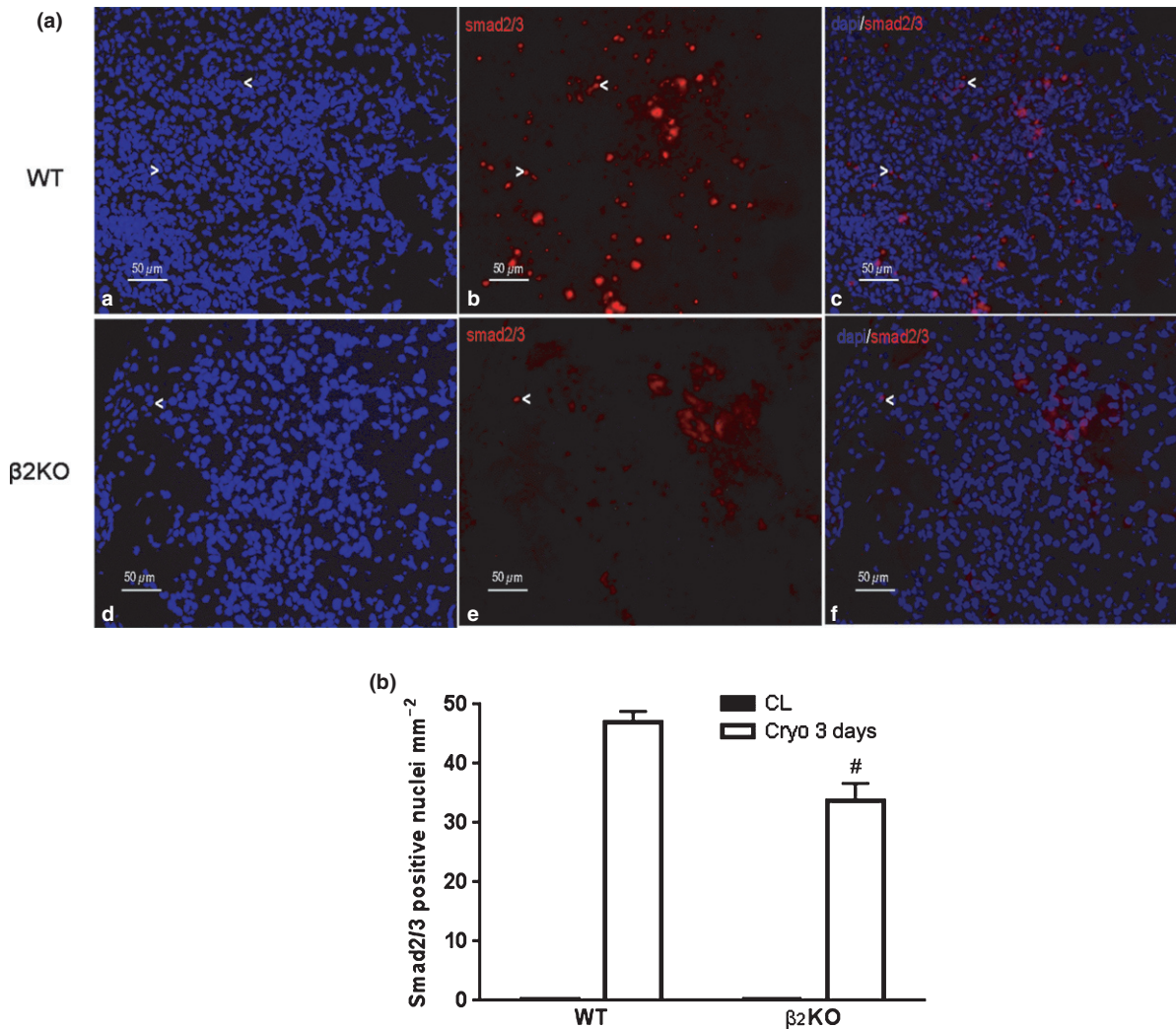
Figure 6 Smad2/3 positive nuclei in muscle cross sections. (a) Immunostaining for Smad2/3 positive nuclei (active Smad2/3) in TA muscle cross sections. TA muscles from WT and β_2KO mice at 3 days post-cryolesion. (a and d) DAPI (blue; stained nuclei) in muscles from WT and β_2KO mice respectively; (b and e) muscles immunostained for Smad2/3 (red; Smad2/3) from WT and β_2KO mice respectively; (c and f) co-staining for active Smad2/3 and DAPI in muscles from WT and β_2KO mice respectively. Arrow heads indicate Smad2/3 positive nuclei. (b) Incidence of Smad2/3 positive nuclei per square millimetre (mm^2) of contralateral muscles and muscles analysed on post-cryolesion day 3 in WT and β_2KO mice. Data are expressed as mean and SD; $n = 3$ (analysis of variance followed by Bonferroni's test for multiple comparisons) [#]$P \leq 0.05$ vs. WT mice.

loss of muscle strength beginning at the 4th contraction stimulus of the fatigue protocol (a 12 and 11% decrease in comparison to the 1st contraction respectively), and that difference persisted up to the 10th contraction ($P \leq 0.05$, Fig. 9). Also, muscle strength at the 1st contraction was significantly lower in the Cryo group than in the contralateral group from both WT and β_2KO mice (39 and 45%, respectively; $P \leq 0.05$, Fig. 9). In the Cryo group from WT and β_2KO mice, muscle strength was also significantly lower at the 4th, 7th and 10th contractions, in comparison with the 1st contraction (WT: 13, 18 and 77% respectively; β_2KO: 11, 19 and 25% respec-

tively; $P \leq 0.05$, Fig. 9). In addition, strength in contralateral and cryolesioned muscles from β_2KO mice decreased when compared to the respective contralateral and cryolesioned muscles from WT mice at all time points (1st, 4th, 7th and 10th) evaluated (CL: 17, 16, 15 and 38% respectively; Cryo: 25, 24, 27 and 27% respectively; $P \leq 0.05$, Fig. 9).

Discussion

Skeletal muscle regeneration is a crucial process responsible for the recovery and maintenance of muscle mass and function. The present study indicated
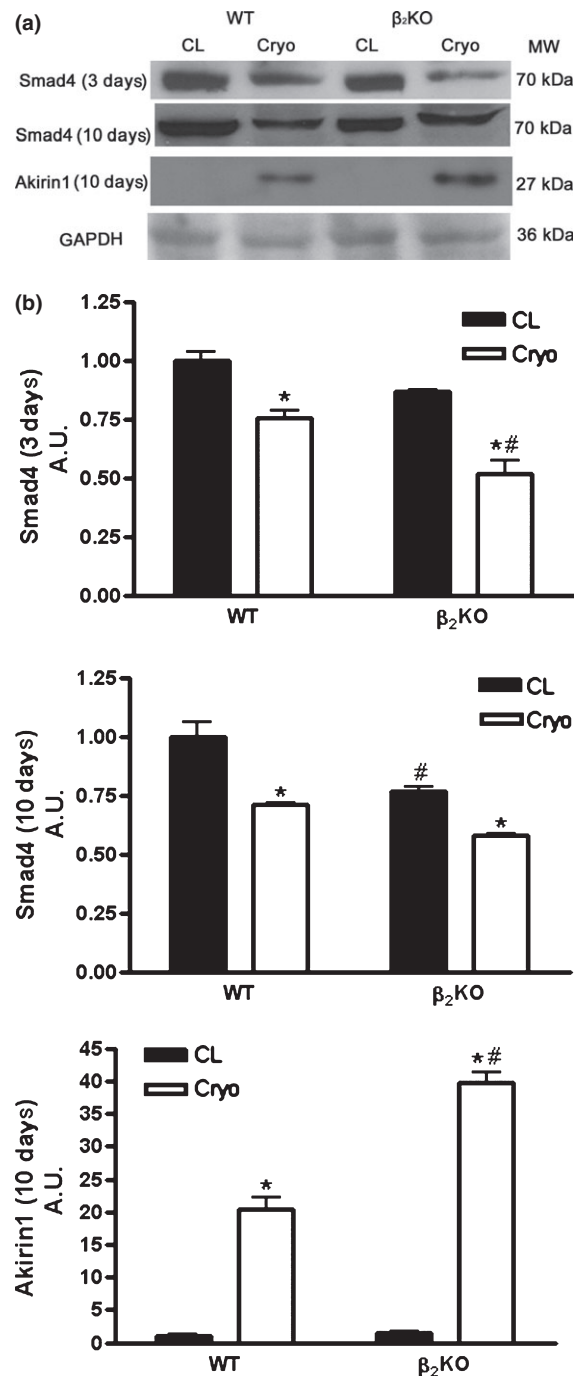
Figure 8 cAMP levels analysed 10 days after cryolesion in WT and β_2KO mice. Data are mean and SD ($n = 7$ muscles per group). CL, contralateral muscle; Cryo, muscle analysed on post-cryolesion day 10. *$P \leq 0.05$ vs. matched CL; [#]$P \leq 0.05$ vs. matched WT group (analysis of variance followed by Bonferroni's test for multiple comparisons).

Figure 7 Smad4 and akirin1 expression. (a) Representative Western blots of contralateral muscles (CL) and injured muscles analysed on post-cryolesion days 3 and 10 (Cryo 3d; Cryo 10d) from WT and β_2KO mice. Blots (50 μg per lane) were reacted with antibodies specific to Smad4 and akirin1 (7 and 12% SDS-PAGE gels respectively), and subsequently with antibody to glyceraldehyde-3-phosphate dehydrogenase (GAPDH), which was used as standard. MW, molecular weight. (b) Densitometry analyses of Smad4 and akirin1. Data are presented as mean and SD of arbitrary unit (A.U.). $n = 3$ (analysis of variance followed by Bonferroni's test for multiple comparisons). *$P \leq 0.05$ vs. CL; [#]$P \leq 0.05$ vs. WT mice.
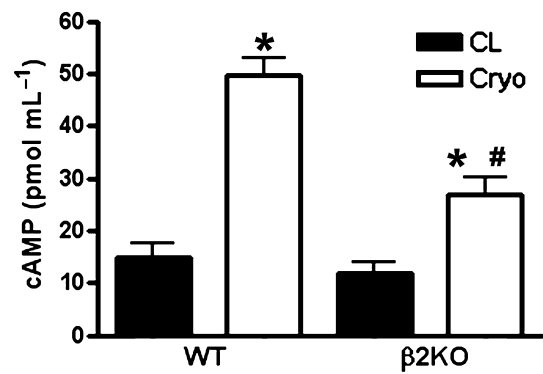
that the β2-adrenoceptor was an important player in this process, as mice lacking this receptor had structural and functional impairments in skeletal muscle regeneration. The time points of 1, 3, 10 and 21 days post-injury were assessed because they represent important phases of skeletal muscle adaptation to injury, including intense necrosis and oedema, inflammation and satellite cell proliferation, evident regeneration with the reestablishment of myofibril proteins, and restoration of the structural and functional features of the skeletal muscle respectively (Hawke & Garry 2001, Miyabara et al. 2006).

Initially, a gain in body weight was observed in β_2KO mice compared to WT mice, suggesting that the β2-adrenoceptor contributed to the regulation of body weight. Notably, this finding is in line with previous studies indicating that β2-adrenergic stimulation causes lipolysis (Louis et al. 2000, Hinkle et al. 2002, Zhang et al. 2007, Lynch & Ryall 2008, Kim & Kong 2010, Kim et al. 2010) and aids in glucose uptake in brown adipocytes from rodents (Marette & Bukowiecki 1990, Shimizu et al. 1996, Chernogubova et al. 2004). The β2-adrenergic agonists are known to induce lipolysis through the activation of Gα-AC-cAMP followed by protein kinase A-mediated phosphorylation of adipose triglyceride lipase, hormone-sensitive-lipase and lipid-bound protein perilipin A; which result in increased hydrolysis of triacylglycerol, diacylglycerol and monoacylglycerol, and the release of free fatty acids from adipocytes (Holm 2003, Pagnon et al. 2012). Therefore, the absence of β2-adrenoceptor may contribute to fat mass accumulation.

With regard to muscle weight, it is interesting to note that β_2KO mice gained less muscle weight at 1 day post-injury, compared to WT mice, which may
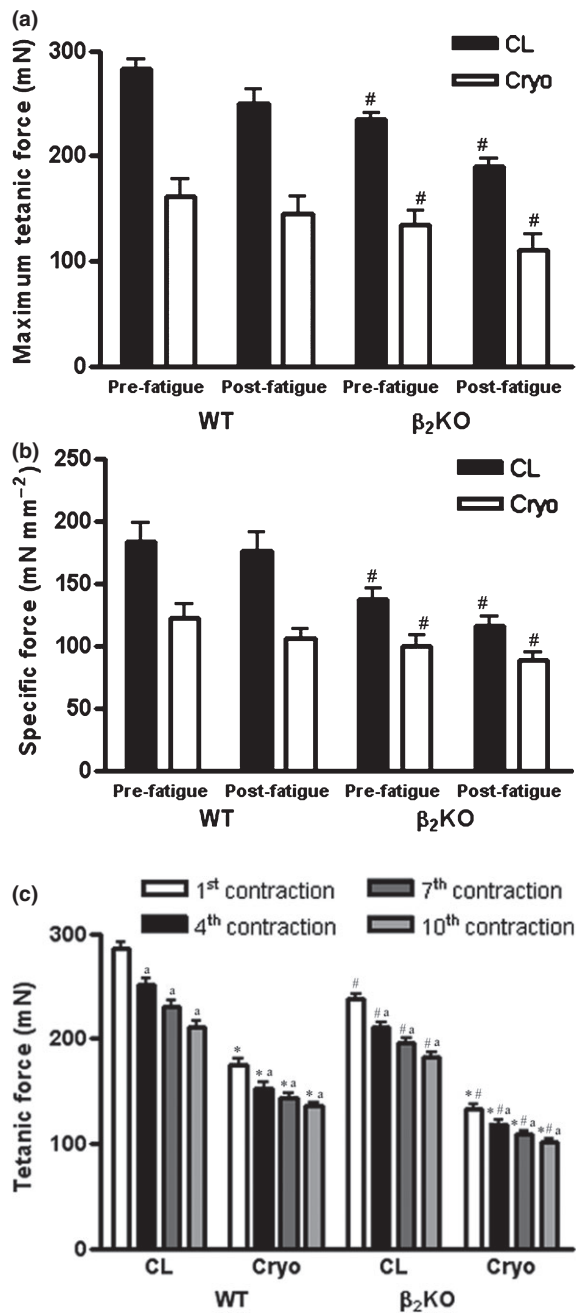
Figure 9 Contractile measurements. (a) Comparison of maximum tetanic force (mN) and (b) specific force in contralateral and cryolesion muscles from WT and β_2KO mice analysed on post-cryolesion day 10. CL, contralateral muscle; Cryo, cryolesioned muscle. Data are expressed as mean and SD; *n* = 8. *$P \leq 0.05$ vs. matched CL; #$P \leq 0.05$ vs. matched WT group; $^a p \leq 0.05$ vs. matched 1 (analysis of variance followed by Bonferroni's test for multiple comparisons). (c) Force production of muscles from WT and β_2KO mice analysed on post-cryolesion day 10 during a protocol of 10 contractions. CL, contralateral muscle; Cryo, cryolesioned muscle. Values are expressed as mean and SD; *n* = 8. *$P \leq 0.05$ vs. matched CL; #$P \leq 0.05$ vs. matched WT group; $^a p \leq 0.05$ vs. the 1st tetanic contraction (mixed models for repeated measures).

be related to a delay in the installation of oedema and inflammation that persisted for 10 days. In agreement with that, other studies have shown that *β2*-adrenoceptor stimulation induces a reduction in inflammation and a better remodelling of the extracellular matrix (Pullar *et al.* 2008, Zhang *et al.* 2010) Therefore, it is probable that the *β2*-adrenoceptor regulates the inflammatory process. In fact, there was a more pronounced increase in the area of inflammation and in the number of macrophages in regenerating muscles lacking the *β2*-adrenoceptor, which led us to investigate possible mechanisms involved in the recruitment of inflammatory cells during muscle regenerative process. In this respect, our data suggest that, in the absence of the *β2*-adrenoceptor, there might be an increase in the frequency of M1 macrophages in regenerating muscles, indicated by a robust increase in iNOS gene expression at 1 day post-injury and a tendency of increase in the number of CD86^{+ve} cells at 3 and 10 days post-injury, which could delay the shift in M1 to M2 macrophage phenotype, and consequently delay the muscle regenerative process. In fact, the shift in M1 to M2 macrophage phenotype is essential for the progression of myogenic differentiation and muscle regeneration (Tsujinaka *et al.* 1996, Szalay *et al.* 1997, Wang *et al.* 2014).

One possible mechanism involved in the shift of M1 to M2 phenotype through the *β2*-adrenoceptor is through cAMP production (Panina-Bordignon *et al.* 1997, Guereschi *et al.* 2013). Accordingly our results indicate that the increase in cAMP levels was attenuated in regenerating myofibres lacking the *β2*-adrenoceptor. However, the downstream signalling mechanisms are not well understood. Another possibility could involve the transactivation of T*β*R-I by the *β2*-adrenoceptor. More specifically, it is known that GPCRs are able to trans-activate serine/threonine kinase receptors (Burch *et al.* 2012), and that akirin1 is a target gene for serine/threonine kinase receptor stimulation (Marshall *et al.* 2008, Salerno *et al.* 2009, Dong *et al.* 2013). Therefore, we hypothesized that the absence of the *β2*-adrenoceptor might inhibit the transactivation of T*β*R-I, and subsequently inhibit its downstream targets, the Smad proteins, which could ultimately lead to increased akirin1 transcription. In fact, we observed a reduced activation of T*β*R-I and Smad2/3 and a decreased Smad4 expression in regenerating muscles lacking the *β2*-adrenoceptor at 3 days post-cryolesion. As a consequence, there was a more pronounced increase in the expression of akirin1, a macrophage chemoattractant, in regenerating muscles lacking the *β2*-adrenoceptor at 10 days post-cryolesion.

Akirin1 expression in macrophages, as well as its chemotactic properties in these cells (Salerno *et al.*

2009), could explain, at least in part, the increased macrophage density and persistence in regenerating muscles lacking the β2-adrenoceptor 10 days post-injury. Akirin1 is also involved in other phases of muscle regeneration and is upregulated in activated satellite cells and in regenerating myofibres (Salerno *et al.* 2009). In addition, akirin1 has been shown to induce post-mitotic differentiation and myotube hypertrophy (Marshall *et al.* 2008), which is in line with our findings on the increased akirin1 expression at 10 days post-cryolesion. Therefore, a higher expression of akirin1 in regenerating muscles lacking the β2-adrenoceptor could also serve as a compensatory mechanism, favouring the muscle regenerative response.

The increase in myofibre size during muscle regeneration seemed to be partially regulated by the β2-adrenoceptor, as demonstrated by a moderate reduction in the calibre of regenerating myofibres from β₂KO mice at 10 days post-cryolesion, when compared to those from WT mice. This result might be explained, to some extent, by the attenuated increase in cAMP levels in regenerating muscles lacking the β2-adrenoceptor. Remarkably, this finding agreed with previous reports indicating that β2-adrenergic stimulation by muscle treatment with β2-agonists after injury led to an increase in both muscular cAMP levels and myofibre calibre (Roberts & McGeachie 1992, Beitzel *et al.* 2004, 2007, Bricout *et al.* 2004, Conte *et al.* 2012), and these effects could be reversed by the β2-antagonist ICI-118551 (Zhong *et al.* 1996, McCormick *et al.* 2010).

With regard to the muscle contraction results, the decreased contractile function in muscles from β2KO mice may be due to impaired contractile mechanisms caused by the absence of the β2-adrenoceptor, rather than to a higher susceptibility to muscle damage, as the β2KO mice had the number of necrotic myofibres similar to those from WT mice. In line with our data, a study indicated that the stimulation of the $Na^+ - K^+$ pump with the β2-adrenoceptor agonist salbutamol, epinephrine, rat calcitonin gene-related peptide (rCGRP), or dibutyryl cAMP, improved force recovery by 40–90% (Mikkelsen *et al.* 2006). In addition, it is known that the β2-adrenergic agonist terbutaline potentiates peak twitch and tetanic force in rat soleus myofibres, which is related to an increase in intracellular free Ca^{2+} ($[Ca^{2+}]_i$) (Ha *et al.* 1999). Considering that this effect is consistent with a mechanism whereby terbutaline activates β2-adrenoceptors leading to the protein kinase A-dependent phosphorylation of ryanodine receptor (Ha *et al.* 1999) with consequent increase in $[Ca^{2+}]_i$ (Cairns *et al.* 1993) and that terbutaline's effect on myofibre force is blocked by the β2-adrenoceptor antagonist ICI 118551; the decreased

absolute and specific tetanic forces found in the TA muscles lacking the β2-adrenoceptor may occur due to an attenuation of protein kinase A-dependent phosphorylation of ryanodine receptor.

The lack of the β2-adrenoceptor, combined with cryolesion, led to much less muscle force production, which might be a consequence of attenuated increase in $[Ca^{2+}]_i$ associated with poor muscle mass recovery in regenerating myofibres under the absence of the β2-adrenoceptor. Muscles lacking the β2-adrenoceptor on post-cryolesion day 10 exhibited a larger area of inflammation and smaller-sized regenerating myofibres compared to those from WT mice. Therefore, it is reasonable to suggest that these muscles contained fewer myofibril components, thereby contributing to the reduction of force output. In line with the effects caused by the absence of β2-adrenoceptors in regenerating skeletal muscle, we have demonstrated that the β2-adrenergic stimulation through formoterol treatment is able to decrease the number of inflammatory cells in regenerating muscles, increase the size of regenerating myofibres, and consequently increase muscle force (Conte *et al.* 2012). In addition, previous studies have also claimed that β2-adrenoceptor stimulation led to improved muscle force generation after injury (Beitzel *et al.* 2004, Ryall *et al.* 2008), which reinforces the hypothesis that the β2-adrenoceptor has a functional importance in muscle regenerative process.

Since there was no difference in the myofibre CSA from β₂KO and WT mice on post-cryolesion day 21, we did not measure muscle function in this time point. Considering that the structure and function of regenerating muscles from β₂KO mice analysed on post-cryolesion day 21 were probably similar to their non-injured contralateral muscles, the β2-adrenoceptor may be involved in the regulation of early phases of the muscle regenerative process, such as inflammation and recovery of myofibre size, and through unknown mechanisms, the delay in these early stages may be compensated.

In summary, this work demonstrates that the β2-adrenoceptor contributes to early stages of muscle regeneration, being particularly involved in the regulation of macrophage recruitment to the regenerating skeletal muscle tissue, possibly through activation of TβR-I and Smad2/3 as well as a reduction in akirin1 expression. Therefore, the β2-adrenoceptor may be an important clinical target for therapeutic interventions with pharmacological agents and gene therapy, with an aim to accelerate the initial phases following muscle injury, and consequently improve recovery and decrease the rehabilitation period in several conditions, such as sports injuries and the damage caused by surgical procedures, accident and frostbite.

Conflicts of interest

The authors declare that they have no conflict of interest.

References

Acharyya, S., Villalta, S.A., Bakkar, N., Bupha-Intr, P., Janssen, P.M.L., Carathers, M., Li, Z., Beg, A.A., Ghosh, S., Sahenk, Z. et al. 2007. Interplay of IKK/NF-κB signaling in macrophages and myofibers promotes muscle degeneration in Duchenne muscular dystrophy. *J Clin Invest* **117**, 889–890.

Aoki, M.S., Soares, A.G., Miyabara, E.H., Baptista, I.L. & Moriscot, A.S. 2009. Expression of genes related to myostatin signaling during rat skeletal muscle longitudinal growth. *Muscle Nerve* **40**, 992–999.

Bancroft, J.D. 1996. *Enzyme Histochemistry*, pp. 391–410. Churchill Living-stone, New York.

Beitzel, F., Gregorevic, P., Ryall, J.G., Plant, D.R., Sillence, M.N. & Lynch, G.S. 2004. Beta2-adrenoceptor agonist fenoterol enhances functional repair of regenerating rat skeletal muscle after injury. *J Appl Physiol* **96**, 1385–1392.

Beitzel, F., Sillence, M.N. & Lynch, G.S. 2007. Beta-Adrenoceptor signaling in regenerating skeletal muscle after beta-agonist administration. *Am J Physiol Endocrinol Metab* **293**, E932–E940.

Blau, H.M., Dhawan, J. & Pavlath, G.K. 1993. Myoblasts in pattern formation and gene therapy. *Trends Genet* **9**, 269–274.

Boldrin, L., Muntoni, F. & Morgan, J.E. 2010. Are human and mouse satellite cells really the same? *J Histochem Cytochem* **58**, 941–955.

Bricout, V.A., Serrurier, B.D. & Bigard, A.X. 2004. Clenbuterol treatment affects myosin heavy chain isoforms and MyoD content similarly in intact and regenerated soleus muscles. *Acta Physiol Scand* **180**, 271–280.

Burch, M.L., Osman, N., Getachew, R., Al-Aryahi, S., Poronnik, P., Zheng, W., Hill, M.A. & Little, P.J. 2012. G protein coupled receptor transactivation: extending the paradigm to include serine/threonine kinase receptors. *Int J Biochem Cell Biol* **44**, 722–727.

Cairns, S.P., Westerblad, H. & Allen, D.G. 1993. Changes of tension and $[Ca^{2+}]_i$ during beta-adrenoceptor activation of single, intact fibres from mouse skeletal muscle. *Pflugers Arch* **425**, 150–155.

Chernogubova, E., Cannon, B. & Bengtsson, T. 2004. Norepinephrine increases glucose transport in brown adipocytes via beta3-adrenoceptors through a cAMP, PKA, and PI3-kinase-dependent pathway stimulating conventional and novel PKCs. *Endocrinology* **145**, 269–280.

Cheung, T.H., Quach, N.L., Charville, G.W., Liu, L., Park, L., Edalati, A., Yoo, B., Hoang, P. & Rando, T.A. 2012. Maintenance of muscle stem-cell quiescence by microRNA-489. *Nature* **482**, 524–528.

Chruscinski, A.J., Rohrer, D.K., Schauble, E., Desai, K.H., Bernstein, D. & Kobilka, B.K. 1999. Targeted disruption of the beta2 adrenergic receptor gene. *J Biol Chem* **274**, 16694–16700.

Ciciliot, S. & Schiaffino, S. 2010. Regeneration of mammalian skeletal muscle. Basic mechanisms and clinical implications. *Curr Pharm Des* **16**, 906–914.

Conte, T.C., Silva, L.H., Silva, M.T., Hirabara, S.M., Oliveira, A.C., Curi, R., Moriscot, A.S., Aoki, M.S. & Miyabara, E.H. 2012. The beta2-adrenoceptor agonist formoterol improves structural and functional regenerative capacity of skeletal muscles from aged rat at the early stages of postinjury. *J Gerontol A Biol Sci Med Sci* **67**, 443–455.

Dong, Y., Pan, J.S. & Zhang, L. 2013. Myostatin suppression of Akirin1 mediates glucocorticoid-induced satellite cell dysfunction. *PLoS One* **8**, e58554.

Droguett, R., Cabello-Verrugio, C., Santander, C. & Brandan, E. 2010. GF-β receptors, in a Smad-independent manner, are required for terminal skeletal muscle differentiation. *Exp Cell Res* **316**, 2487–2503.

Drummond, M.J., Dreyer, H.C., Fry, C.S., Glynn, E.L. & Rasmussen, B.B. 2009. Nutritional and contractile regulation of human skeletal muscle protein synthesis and mTORC1 signaling. *J Appl Physiol* **106**, 1374–1384.

Ferrari, G., Cusella-De Angelis, G., Coletta, M., Paolucci, E., Stornaiuolo, A., Cossu, G. & Mavilio, F. 1998. Muscle regeneration by bone marrow-derived myogenic progenitors. *Science* **279**, 1528–1530.

Ge, Y., Wu, A.L., Warnes, C., Liu, J., Zhang, C., Kawasome, H., Terada, H., Boppart, M.D., Schoenherr, C.J. & Chen, J. 2009. mTOR regulates skeletal muscle regeneration in vivo through kinase-dependent and kinase-independent mechanisms. *Am J Physiol Cell Physiol* **297**, C1434–C1444.

Guereschi, M.G., Araujo, L.P., Maricato, J.T., Takenaka, M.C., Nascimento, V.M., Vivanco, B.C., Reis, V.O., Keller, A.C., Brum, P.C. & Basso, A.S. 2013. Beta2-adrenergic receptor signaling in CD4⁺Foxp3⁺ regulatory T cells enhances their suppressive function in a PKA-dependent manner. *Eur J Immunol* **43**, 1001–1012.

Ha, T.N., Posterino, G.S. & Fryer, M.W. 1999. Effects of terbutaline on force and intracellular calcium in slow-twitch skeletal muscle fibres of the rat. *Br J Pharmacol* **126**, 1717–1724.

Hawke, T.J. & Garry, D.J. 2001. Myogenic satellite cells: physiology to molecular biology. *J Appl Physiol* **91**, 534–551.

Hinkle, R.T., Hodge, K.M., Cody, D.B., Sheldon, R.J., Kobilka, B.K. & Isfort, R.J. 2002. Skeletal muscle hypertrophy and anti-atrophy effects of clenbuterol are mediated by the beta2-adrenergic receptor. *Muscle Nerve* **25**, 729–734.

Holm, C. 2003. Molecular mechanisms regulating hormone-sensitive lipase and lipolysis. *Biochem Soc Trans* **31**, 1120–1124.

Karpati, G., Carpenter, S. & Prescott, S. 1988. Small-caliber skeletal muscle fibers do not suffer necrosis in mdx mouse dystrophy. *Muscle Nerve* 11, 795–803.

Kim, S.K. & Kong, C.S. 2010. Anti-adipogenic effect of dioxinodehydroeckol via AMPK activation in 3T3-L1 adipocytes. *Chem Biol Interact* 186, 24–29.

Kim, Y.S., Sainz, R.D., Molenaar, P. & Summers, R.J. 1991. Characterization of beta 1- and beta 2-adrenoceptors in rat skeletal muscles. *Biochem Pharmacol* 42, 1783–1789.

Kim, H.K., Della-Fera, M.A., Hausman, D.B. & Baile, C.A. 2010. Effect of clenbuterol on apoptosis, adipogenesis, and lipolysis in adipocytes. *J Physiol Biochem* 66, 197–203.

Kline, W.O., Panaro, F.J., Yang, H. & Bodine, S.C. 2007. Rapamycin inhibits the growth and muscle-sparing effects of clenbuterol. *J Appl Physiol* 102, 740–747.

Krause, M.P., Moradi, J., Coleman, S.K., D'Souza, D.M., Liu, C., Kronenberg, M.S., Rowe, D.W., Hawke, T.J. & Hadjiargyrou, M. 2013. A novel GFP reporter mouse reveals Mustn1 expression in adult regenerating skeletal muscle, activated satellite cells and differentiating myoblasts. *Acta Physiol* 208, 180–190.

Larocca, R.A., Moraes-Vieira, P.M., Bassi, E.J., Semedo, P., de Almeida, D.C., da Silva, M.B., Thornley, T., Pacheco-Silva, A. & Câmara, N.O. 2013. Adipose tissue-derived mesenchymal stem cells increase skin allograft survival and inhibit Th-17 immune response. *PLoS One* 8, e76396.

Locati, M., Mantovani, A. & Sica, A. 2013. Macrophage activation and polarization as an adaptive component of innate immunity. *Adv Immunol* 120, 163–184.

Louis, S.N., Jackman, G.P., Nero, T.L., Iakovidis, D. & Louis, W.J. 2000. Role of beta-adrenergic receptor subtypes in lipolysis. *Cardiovasc Drugs Ther* 14, 565–577.

Lynch, G.S. & Ryall, J.G. 2008. Role of beta-adrenoceptor signaling in skeletal muscle: implications for muscle wasting and disease. *Physiol Rev* 88, 729–767.

Mantovani, A., Biswas, S.K., Galdiero, M.R., Sica, A. & Locati, M. 2013. Macrophage plasticity and polarization in tissue repair and remodelling. *J Pathol* 229, 176–185.

Marette, A. & Bukowiecki, L.J. 1990. Mechanism of norepinephrine stimulation of glucose transport in isolated rat brown adipocytes. *Int J Obes* 14, 857–867.

Marshall, A., Salerno, M.S., Thomas, M., Davies, T., Berry, C., Dyer, K., Bracegirdle, J., Watson, T., Dziadek, M., Kambadur, R., Bower, R. & Sharma, M. 2008. Mighty is a novel promyogenic factor in skeletal myogenesis. *Exp Cell Res* 314, 1013–1029.

McCormick, C., Alexandre, L., Thompson, J. & Mutungi, G. 2010. Clenbuterol and formoterol decrease force production in isolated intact mouse skeletal muscle fiber bundles through a beta2-adrenoceptor-independent mechanism. *J Appl Physiol* 109, 1716–1727.

Mikkelsen, U.R., Gissel, H., Fredsted, A. & Clausen, T. 2006. Excitation-induced cell damage and beta2-adrenoceptor agonist stimulated force recovery in rat skeletal muscle. *Am J Physiol Regul Integr Comp Physiol* 290, R265–R272.

Miyabara, E.H., Tostes, R.C., Selistre de Araujo, H.S., Aoki, M.S., Salvini, T.F. & Moriscot, A.S. 2004. Cyclosporin A attenuates skeletal muscle damage induced by crotoxin in rats. *Toxicon* 43, 35–42.

Miyabara, E.H., Martin, J.L., Griffin, T.M., Moriscot, A.S. & Mestril, R. 2006. Overexpression of inducible 70-kDa heat shock protein in mouse attenuates skeletal muscle damage induced by cryolesioning. *Am J Physiol Cell Physiol* 290, C1128–C1138.

Miyabara, E.H., Conte, T.C., Silva, M.T., Baptista, I.L., Bueno, C. Jr, Fiamoncini, J., Lambertucci, R.H., Serra, C.S., Brum, P.C., Pithon-Curi, T., Aoki, M.S., Oliveira, A.C. & Moriscot, A.S. 2010. Mammalian target of rapamycin complex 1 is involved in differentiation of regenerating myofibers in vivo. *Muscle Nerve* 42, 778–787.

Navegantes, L.C., Resano, N.M., Migliorini, R.H. & Kettelhut, I.C. 2000. Role of adrenoceptors and cAMP on the catecholamine-induced inhibition of proteolysis in rat skeletal muscle. *Am J Physiol Endocrinol Metab* 279, E663–E668.

Navegantes, L.C., Migliorini, R.H. & do Carmo Kettelhut, I. 2002. Adrenergic control of protein metabolism in skeletal muscle. *Curr Opin Clin Nutr Metab Care* 5, 281–286.

Pagnon, J., Matzaris, M., Stark, R., Meex, R.C., Macaulay, S.L., Brown, W., O'Brien, P.E., Tiganis, T. & Watt, M.J. 2012. Identification and functional characterization of protein kinase A phosphorylation sites in the major lipolytic protein, adipose triglyceride lipase. *Endocrinology* 153, 4278–4289.

Panina-Bordignon, P., Mazzeo, D., Di Lucia, P., D'Ambrosio, D., Lang, R., Fabbri, L., Self, C. & Sinigaglia, F. 1997. *β*2-Agonists prevent Th1 development by selective inhibition of interleukin 12. *J Clin Invest* 100, 1513–1519.

Pereira, M.G., Baptista, I.L., Carlassara, E.O., Moriscot, A.S., Aoki, M.S. & Miyabara, E.H. 2014. Leucine supplementation improves skeletal muscle regeneration after cryolesion in rats. *PLoS One* 9, e85283.

Persson, P.B. 2013. Good publication practice in physiology. Guidelines for Acta Physiologica. *Acta Physiol* 209, 250–253.

Pullar, C.E., Manabat-Hidalgo, C.G., Bolaji, R.S. & Isseroff, R.R. 2008. beta-Adrenergic receptor modulation of wound repair. *Pharmacol Res* 58, 158–164.

Roberts, P. & McGeachie, J.K. 1992. The effects of clenbuterol on satellite cell activation and the regeneration of skeletal muscle: an autoradiographic and morphometric study of whole muscle transplants in mice. *J Anat* 180, 57–65.

Roberts, P. & McGeachie, J.K. 1994. The enhancement of revascularisation of skeletal muscle transplants using the beta 2-agonist isoprenaline. *J Anat* 184, 309–318.

Ryall, J.G., Schertzer, J.D., Alabakis, T.M., Gehrig, S.M., Plant, D.R. & Lynch, G.S. 2008. Intramuscular beta2-agonist administration enhances early regeneration and functional repair in rat skeletal muscle after myotoxic injury. *J Appl Physiol* 105, 165–172.

Salerno, M.S., Dyer, K., Bracegirdle, J., Platt, L., Thomas, M., Siriett, V., Kambadur, R. & Sharma, M. 2009. Akirin1 (Mighty), a novel promyogenic factor regulates muscle regeneration and cell chemotaxis. *Exp Cell Res* 315, 2012–2021.

Shimizu, Y., Kielar, D., Minokoshi, Y. & Shimazu, T. 1996. Noradrenaline increases glucose transport into brown adipocytes in culture by a mechanism different from that of insulin. *Biochem J* **314**, 485–490.

Silva, L.H., Silva, M.T., Gutierrez, R.M., Conte, T.C., Toledo, C.A., Aoki, M.S., Liebano, R.E. & Miyabara, E.H. 2012. GaAs 904-nm laser irradiation improves myofiber mass recovery during regeneration of skeletal muscle previously damaged by crotoxin. *Lasers Med Sci* **27**, 993–1000.

Spurlock, D.M., McDaneld, T.G. & McIntyre, L.M. 2006. Changes in skeletal muscle gene expression following clenbuterol administration. *BMC Genomics* **7**, 320.

Stipanuk, M.H. 2007. Leucine and protein synthesis: mTOR and beyond. *Nutr Rev* **65**, 122–129.

Szalay, K., Razga, Z. & Duda, E. 1997. TNF inhibits myogenesis and downregulates the expression of myogenic regulatory factors myoD and myogenin. *Eur J Cell Biol* **74**, 391–398.

Ten Broek, R.W., Grefte, S. & Von den Hoff, J.W. 2010. Regulatory factors and cell populations involved in skeletal muscle regeneration. *J Cell Physiol* **224**, 7–16.

Tsivitse, S. 2010. Notch and Wnt signaling, physiological stimuli and postnatal myogenesis. *Int J Biol Sci* **6**, 268–281.

Tsujinaka, T., Fujita, J., Ebisui, C., Yano, M., Kominami, E., Suzuki, K., Tanaka, K., Katsume, A., Ohsugi, Y., Shiozaki, H. & Monden, M. 1996. Interleukin 6 receptor antibody inhibits muscle atrophy and modulates proteolytic systems in interleukin 6 transgenic mice. *J Clin Invest* **97**, 244–249.

Turner, N.J. & Badylak, S.F. 2012. Regeneration of skeletal muscle. *Cell Tissue Res* **347**, 759–774.

Vary, T.C. & Lynch, C.J. 2007. Nutrient signaling components controlling protein synthesis in striated muscle. *J Nutr* **137**, 18351–1843.

Villalta, S.A., Deng, B., Rinaldi, C., Wehling-Henricks, M. & Tidball, J.G. 2011. IFN-γ promotes muscle damage in the mdx mouse model of Duchenne muscular dystrophy by suppressing M2 macrophage activation and inhibiting muscle cell proliferation. *J Immunol* **187**, 5419–5428.

Wang, H., Melton, D., Porter, L., Sarwar, Z.U., McManus, L.M. & Shireman, P.K. 2014. Altered macrophage-phenotype transition impairs skeletal muscle regeneration. *Am J Pathol* **184**, 1167–1184.

Zhang, J., He, Q., Liu, Q.Y., Guo, W., Deng, X.M., Zhang, W.W., Hu, X.X. & Li, N. 2007. Differential gene expression profile in pig adipose tissue treated with/without clenbuterol. *BMC Genomics* **8**, 433.

Zhang, W., Fievez, L., Cheu, E., Bureau, F., Rong, W., Zhang, F., Zhang, Y., Advenier, C. & Gustin, P. 2010. Anti-inflammatory effects of formoterol and ipratropium bromide against acute cadmium-induced pulmonary inflammation in rats. *Eur J Pharmacol* **628**, 171–178.

Zhong, H., Guerrero, S.W., Esbenshade, T.A. & Minneman, K.P. 1996. Inducible expression of beta 1- and beta 2-adrenergic receptors in rat C6 glioma cells: functional interactions between closely related subtypes. *Mol Pharmacol* **50**, 175–184.

Zhu, J., Li, Y., Lu, A., Gharaibeh, B., Ma, J., Kobayashi, T., Quintero, A.J. & Huard, J. 2011. Follistatin improves skeletal muscle healing after injury and disease through an interaction with muscle regeneration, angiogenesis, and fibrosis. *Am J Pathol* **179**, 915–930.